




Androgen signaling stabilizes genomes to counteract senescence by promoting XRCC4 transcription

Yu Chen^{1,2,†} , Zhengyi Zhen^{1,2,†}, Lingjiang Chen^{1,2,†}, Hao Wang^{1,2}, Xuhui Wang^{1,2}, Xiaoxiang Sun^{1,2}, Zhiwei Song^{1,2}, Haiyan Wang^{1,2}, Yizi Lin¹ , Wenjun Zhang³, Guizhu Wu⁴, Ying Jiang^{1,*} & Zhiyong Mao^{2,**} 

Abstract

Aging is accompanied by a decreased DNA repair capacity, which might contribute to age-associated functional decline in multiple tissues. Disruption in hormone signaling, associated with reproductive organ dysfunction, is an early event of age-related tissue degeneration, but whether it impacts DNA repair in nonreproductive organs remains elusive. Using skin fibroblasts derived from healthy donors with a broad age range, we show here that the downregulation of expression of XRCC4, a factor involved in nonhomologous end-joining (NHEJ) repair, which is the dominant pathway to repair somatic double-strand breaks, is mediated through transcriptional mechanisms. We show that the androgen receptor (AR), whose expression is also reduced during aging, directly binds to and enhances the activity of the XRCC4 promoter, facilitating XRCC4 transcription and thus stabilizing the genome. We also demonstrate that dihydrotestosterone (DHT), a powerful AR agonist, restores XRCC4 expression and stabilizes the genome in different models of cellular aging. Moreover, DHT treatment reverses senescence-associated phenotypes, opening a potential avenue to aging interventions in the future.

Keywords aging; androgen receptor; dihydrotestosterone; DNA repair; XRCC4

Subject Categories Chromatin, Transcription & Genomics; DNA Replication, Recombination & Repair

DOI 10.15252/embr.202356984 | Received 13 February 2023 | Revised 16 October 2023 | Accepted 24 October 2023 | Published online 13 November 2023

EMBO Reports (2023) 24: e56984

Introduction

Genomic instability is a fundamental hallmark of aging, and inefficient or unfaithful DNA repair is the major reason for the loss of genome integrity. DNA damage has been shown to accumulate with increasing age in mammals (di Fagagna *et al*, 2003; Sedelnikova *et al*, 2004, 2008; Liu *et al*, 2005; Wang *et al*, 2009; Zhang *et al*, 2020; Gladyshev *et al*, 2021; Aging Biomarker Consortium *et al*, 2023), studies on age-related changes in DNA repair and underlying mechanisms causing these alterations in humans are very rare, possibly due to the difficulties in obtaining the human materials needed and the lack of appropriate tools to quantify repair efficiency. Using eyelid fibroblasts isolated from healthy female donors of different ages and a well-characterized, fluorescence-based reporter system, in our previous study, we demonstrated that the efficiency of nonhomologous end-joining (NHEJ), the predominant double-strand break repair pathway in somatic cells, showed significant age-associated decline arising from decreased protein expression levels of XRCC4 and Lig4 (Li *et al*, 2016). Nevertheless, how the expression of DNA repair factors changes with age remains to be determined.

Increasing evidence has shown that the amount of circulating sex hormones decreases with age (Lamberts *et al*, 1997), which reflects an important aspect of reproductive aging. Among all human organs, reproductive organs are the first to exhibit age-related dysfunction (Duncan *et al*, 2018). From the viewpoint of the evolution of aging, the gradual loss of reproductive function with increasing age is a reasonable adjustment to the investment of energy. However, whether aging of the reproductive system adversely impacts other organs, possibly by modulating the composition of circulating hormones, thereby further initiating systemic aging, is an intriguing topic to be explored. Moreover, sex hormones bind to and regulate

1 Yangzhi Rehabilitation Hospital (Shanghai Sunshine Rehabilitation Center), Shanghai Key Laboratory of Signaling and Disease Research, School of Life Sciences and Technology, Tongji University, Shanghai, China

2 Shanghai Key Laboratory of Maternal Fetal Medicine, Clinical and Translational Research Center of Shanghai First Maternity and Infant Hospital, Frontier Science Center for Stem Cell Research, School of Life Sciences and Technology, Tongji University, Shanghai, China

3 Department of Plastic Surgery, Changzheng Hospital, Shanghai, China

4 Department of Gynecology, Shanghai First Maternity and Infant Hospital, Shanghai Tongji University School of Medicine, Shanghai, China

*Corresponding author. Tel: +86 21 65978166; Fax: +86 21 65981041; E-mail: ying_jiang@tongji.edu.cn

**Corresponding author. Tel: +86 21 65978166; Fax: +86 21 65981041; E-mail: zhiyong_mao@tongji.edu.cn

†These authors contributed equally to this work

the activity of sex hormone receptors (Shang *et al*, 2002; Schaufele *et al*, 2005). Whether these sex hormone receptors, which show widespread expression in nonreproductive tissues (White & Porterfield, 2013), also undergo age-related alterations and whether these potential changes contribute to the aging process of the tissues in which they are expressed remain to be determined.

Cellular senescence is another hallmark of individual aging (Lopez-Otin *et al*, 2013). Impaired DNA repair has been linked to the onset of cellular senescence, which plays a critical role in the development of age-related diseases (Chen *et al*, 2020). Cellular senescence triggers the production and secretion of a variety of extracellular modulators, including cytokines, chemokines, and proteases, referred to as the senescence-associated secretory phenotype (SASP) (Coppe *et al*, 2010). The SASP has been reported to function in both an autocrine manner to reinforce the cell cycle arrest state of senescent cells (Kortlever *et al*, 2006; Acosta *et al*, 2008) and a paracrine manner to reconstitute the microenvironment and impact the fate of nearby cells (Krtolica *et al*, 2001; Hoare & Narita, 2013), mediating the propagation of cellular senescence and tumor progression. This evidence strongly suggests that the SASP might serve as a prominent mediator of systemic aging. Although DNA damage *per se* contributes to the secretion of SASP factors (Rodier *et al*, 2009; Yu *et al*, 2015), whether the specific rescue of the age-related decline in DNA repair can be leveraged to suppress the onset of cellular senescence and thus inhibit SASP and its potential deleterious consequences remains unclear.

In this study, we showed that the androgen receptor (AR), a transcription factor, directly bound to the XRCC4 promoter to activate its transcription and that age-associated downregulation of AR led to the loss of XRCC4 protein expression in human skin fibroblasts. Moreover, AR-mediated regulation of XRCC4 expression was shown to play a vital role in stabilizing the genome and protecting cells from stress-induced premature senescence (SIPS). Additionally, we showed that supplementation of cell cultures with dihydrotestosterone (DHT), a specific AR agonist, reversed the decline in XRCC4 expression, stabilized the genome, and suppressed the onset of radiation-induced cellular senescence in cells derived from physiologically aged individuals or Hutchinson–Gilford progeria syndrome (HGPS) patients. Moreover, DHT treatment significantly suppressed the SASP, suggesting a novel method to combat systemic aging in the future.

Results

XRCC4 transcription declines with age

Using a large panel of eyelid fibroblast cell lines isolated from healthy female donors, our previous study has reported that the protein levels of XRCC4 and Lig4 exhibit significant age-related downregulation (Li *et al*, 2016). To investigate whether the age-related decrease in XRCC4 and Lig4 protein levels is attributable to altered mRNA levels, total RNA was extracted from previously characterized fibroblasts. All the 14 primary cells (7 young versus 7 old) used for the analysis were in population-doubling number 16–19. Real-time qPCR results showed that XRCC4 mRNA levels were significantly decreased, by 34.9%, in the group of aged cells compared to the group of young cells (Fig 1A and B). A correlation analysis

revealed that the XRCC4 mRNA level was negatively correlated with age ($R^2 = 0.4409$, $P = 0.0096$) (Fig EV1A). However, the mRNA level of Lig4 was not significantly different between the young and old cell groups (Fig 1C and D). Since it had been reported that XRCC4 stabilizes the Lig4 protein (Bryans *et al*, 1999), we reasoned that the decrease in Lig4 protein level that we observed in aged eyelid fibroblasts might have been a result of the downregulation of XRCC4 expression. Moreover, the age-associated downregulation in XRCC4 mRNA level was confirmed by data mining of the GTEx database. *In silico* analysis demonstrated that the mRNA level of XRCC4 was significantly lower in multiple tissues, including hearts, brains, blood, stomachs, small intestines, and ovaries, in the aged humans than those in the young individuals (Fig EV1B–G).

Next, to examine whether the decline in mRNA levels was caused by a reduction in the transcription rate, we fused the promoter of XRCC4 with a firefly luciferase gene (Fig 1E). A dual-luciferase reporter assay demonstrated that the XRCC4 promoter activity was significantly decreased by 62.1% in the aged cells compared to the young cells (Fig 1F), and a significant negative correlation was found between XRCC4 promoter activity and age ($R^2 = 0.6883$, $P = 0.0002$) (Fig 1G). Consistent with the mRNA data, the activity of the Lig4 promoter was not altered in the aged group (Fig EV1H and I), and no significant correlation was identified between Lig4 promoter activity and age (Fig EV1J). Moreover, our data indicated that XRCC4 promoter activity was positively correlated with XRCC4 mRNA levels ($R^2 = 0.3317$, $P = 0.0311$) (Fig 1H), suggesting that decreased transcriptional activity might lead to decreased XRCC4 mRNA levels during aging.

The androgen receptor (AR) binds to the XRCC4 promoter and activates XRCC4 gene transcription

To identify the factor(s) critical to the age-related downregulation of XRCC4 transcription, we predicted transcription factors that potentially bind to the XRCC4 promoter using the PROMO 3.0 program (Messeguer *et al*, 2002; Farre *et al*, 2003). Interestingly, we noticed that several steroid hormone receptors, including glucocorticoid receptor (GR), estrogen receptor (ER), AR, and progesterone receptor (PR), were putative factors that bind to the XRCC4 promoter (Fig 2A). Since dysregulation of hormone signaling is associated with aging of individual (Lamberts *et al*, 1997; Kaufman & Vermeulen, 2005), we first set out to confirm whether the aforementioned receptors were downregulated in aged cells. Real-time qPCR analysis revealed that the mRNA level of AR, but not that GR, ER, or PR, was significantly downregulated in the group of aged cells (Figs 2B and EV2A–C), indicating an unexpected but important role of androgenic signaling in the regulation of female aging. Western blot analysis confirmed that the protein level of AR declined in the aged cell group (Fig 2C and D), and consistent with our previous report (Li *et al*, 2016), the protein levels of XRCC4 and Lig4 decreased with age (Fig EV2D and E). Moreover, both the mRNA and protein levels of AR showed a significant inverse correlation with age (Figs 2E and EV2F).

More importantly, the AR protein level positively correlated with the XRCC4 mRNA level, protein level, and promoter activity (Figs 2F and EV2G and H), indicating a potential regulatory role for AR in XRCC4 expression. To explore whether AR, a transcription factor, directly binds to the promoter of XRCC4, a CHIP-qPCR assay

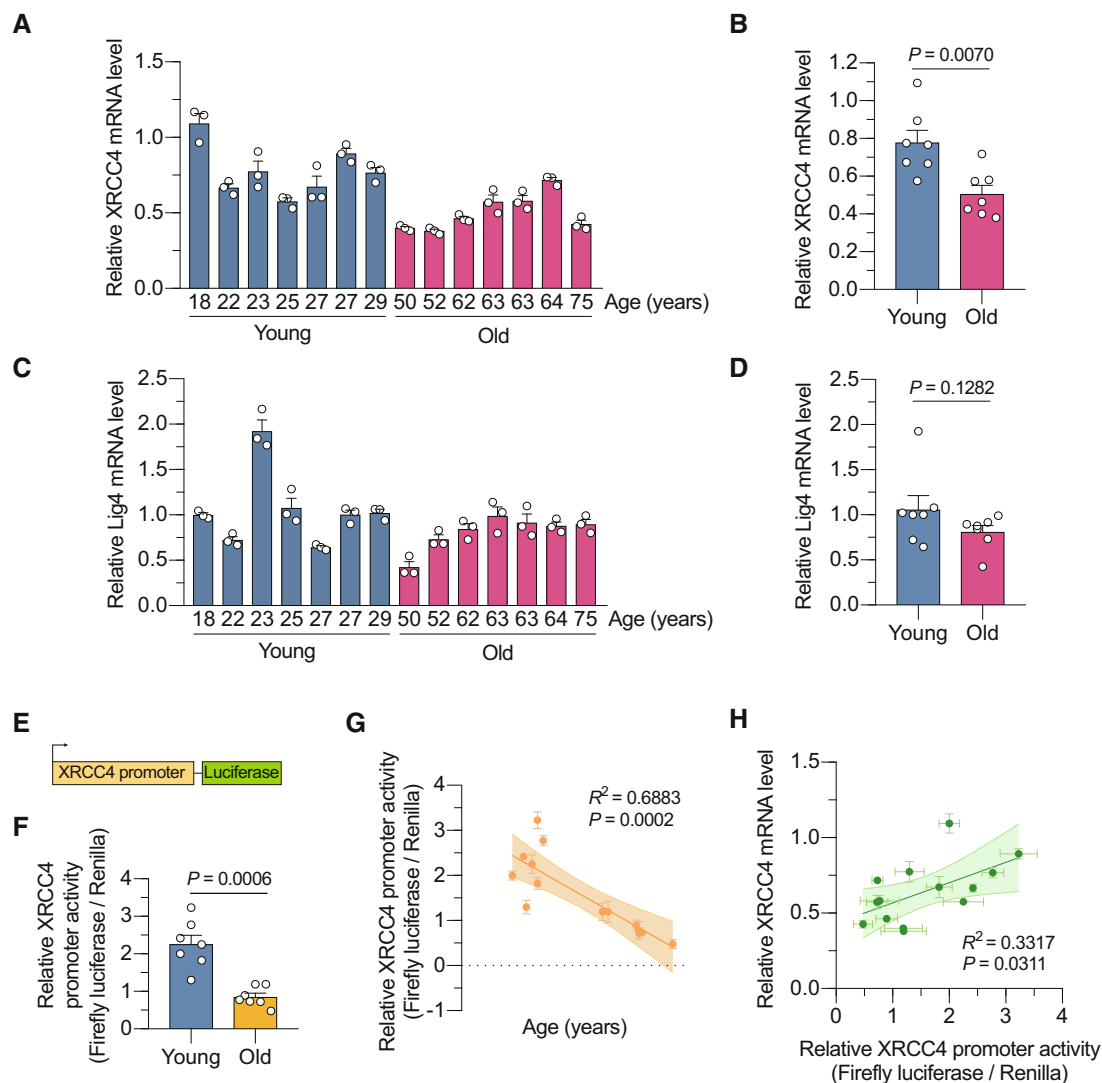


Figure 1. Age-associated downregulation of XRCC4 promoter activity and transcription contribute to reduced XRCC4 expression.

- A Real-time qPCR analysis of the relative mRNA level of XRCC4 (normalized to GAPDH mRNA level) in eyelid fibroblasts derived from 7 young versus 7 old donors.
- B Statistical comparison of relative XRCC4 mRNA levels between the young and old group. Each dot represents one donor. $n = 7$ biological replicates.
- C Real-time qPCR analysis of the relative mRNA level of Lig4 (normalized to GAPDH mRNA level) in eyelid fibroblasts derived from 7 young versus 7 old donors.
- D Statistical comparison of relative Lig4 mRNA levels between the young and old group. Each dot represents one donor. $n = 7$ biological replicates.
- E Schematic diagram of the luciferase reporter driven by XRCC4 promoter.
- F Analysis of the XRCC4 promoter activity in the young and old group with the dual-luciferase reporter system. Renilla luciferase was used as the internal control. $n = 7$ biological replicates.
- G Correlation between the relative XRCC4 promoter activity and donor age.
- H Correlation between the relative XRCC4 promoter activity and relative XRCC4 mRNA level.

All the experiments were repeated for at least three times. Mann–Whitney U test was performed to determine the significance of the results presented in (B), (D), (F), and t test was performed to assess the significance of the regression slope in (G) and (H). Error bars represent the s.e.m. values in (A) to (D), and (F) to (H). Source data are available online for this figure.

was performed. Seven pairs of primers were designed on the basis of the XRCC4 promoter to specifically amplify sequences flanking the eight putative AR-binding sites predicted via the PROMO 3.0 program (Fig 2G). The results indicated that AR bound to the XRCC4 promoter in the region from -238 to -68 (Fig 2H). The result was confirmed by ChIP-qPCR assay with an antibody against the endogenous AR (Fig 2I). To investigate whether AR regulates XRCC4 promoter activity, a luciferase assay was carried out. The data showed

that depleting AR significantly impaired XRCC4 promoter activity, while reintroducing AR expression into AR-knockdown cells reactivated the promoter (Fig 2J). To further study whether AR directly regulates XRCC4 promoter activity, a truncated XRCC4 promoter within the region spanning from -238 to -68 deleted or with the potential AR-binding site (-166 to -158) removed was created and fused to a luciferase reporter vector (Figs 2K and EV21). Consistent with our ChIP-qPCR results, AR overexpression enhanced the

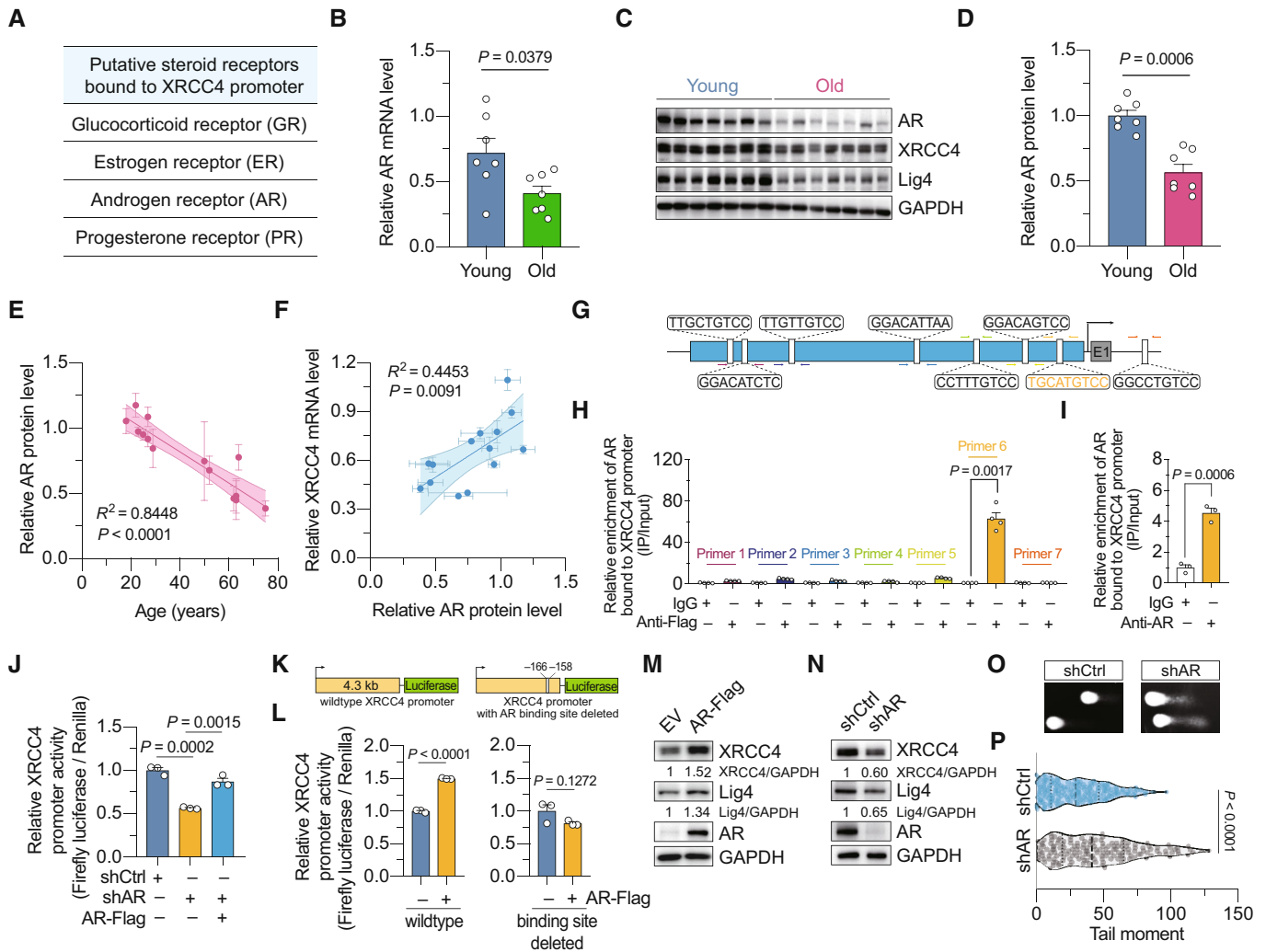


Figure 2. Age-related AR downregulation impairs its stimulatory effect on XRCC4 expression as a transcription factor.

- A** Putative transcription factors bound to XRCC4 promoter predicted with PROMO algorithm.
- B** Comparison of the relative AR mRNA level (normalized to GAPDH mRNA level) in cells derived from young and aged individuals. $n = 7$ biological replicates.
- C** Analysis of the protein expression level of AR, XRCC4, and Lig4 in the cells derived from young and aged individuals, by Western blot.
- D** Quantification of the gray scale of AR protein level. Each dot represents the average relative gray scale value of AR (normalized to the gray scale of GAPDH), assayed by three independent repeats of Western blot, for one donor.
- E** Correlation between the relative AR protein level and donor age. $n = 14$ donors.
- F** Correlation between the relative AR protein level and relative XRCC4 mRNA level. $n = 14$ donors.
- G** Illustration of the predicted AR-binding sites on XRCC4 promoter. Arrows indicate the seven pairs of primers designed for amplifying the sequences flanking the eight predicted AR-binding sites.
- H** ChIP-qPCR analysis of relative AR enrichment to the predicted binding sites on XRCC4 promoter. Flag-tagged AR was transfected into cells, and immunoprecipitation was performed with anti-Flag or IgG. $n = 4$ biological replicates.
- I** ChIP-qPCR analysis of the enrichment of endogenous AR to XRCC4 promoter. $n = 3$ biological replicates.
- J** Analysis of XRCC4 promoter activity in HCA2-hTERT cells integrated with shRNA against AR, and cells were transfected with empty vector or vectors encoding AR to restoring AR expression. $n = 3$ biological replicates.
- K** Schematic diagrams of the firefly luciferase reporter driven by the wild-type XRCC4 promoter and the promoter with AR-binding site TGCATGTCC (-166 bp to -158 bp) deleted.
- L** The effect of AR overexpression on XRCC4 promoter activity, assayed with the two luciferase reporters in (K). $n = 3$ biological replicates.
- M** The effect of AR overexpression on the protein level of XRCC4 and Lig4. EV, empty vector.
- N** The effect of AR knockdown on the protein level of XRCC4 and Lig4.
- O, P** The effect of shRNA-mediated knockdown of AR on the genomic stability in HCA2-hTERT cells, analyzed by comet assay. Each dot represents one comet analyzed ($n =$ at least 150 cells). Representative comet images are shown in (O), and the quantitative result is shown in (P).

Error bars represent the s.e.m. values in (B), (D) to (F), (H) to (J), and (L). Mann-Whitney U test was performed to determine the significance of the results presented in (B), (D), and (P), unpaired t test was performed to determine the significance of the results presented in (H), (I), (J), and (L), and t test was performed to assess the significance of the regression slope in (E) and (F).

Source data are available online for this figure.

activity of the wild-type XRCC4 promoter but exerted no stimulatory effect on the activity of the truncated XRCC4 promoter in which the -238 to -68 region was deleted (Fig EV2J) or in which the AR-binding site was deleted (Fig 2L). Therefore, overexpression of AR led to elevated expression of XRCC4 and Lig4 (Fig 2M), while shRNA-mediated depletion of AR reduced the protein levels of XRCC4 and Lig4 (Fig 2N). Our previous study showed that reduced XRCC4 and Lig4 expression led to genomic instability (Li et al, 2016). Therefore, a comet assay was performed to assess the effect of AR depletion on genomic stability, and the data showed that AR knockdown in HCA2-hTERT cells significantly increased the tail moment, reflecting a destabilized genome (Figs 2O and P, EV2K and L). Taken together, our data suggest that AR binds to and activates the promoter of XRCC4 to stimulate XRCC4 transcription, thereby improving genomic stability. Interestingly, using the AgeAnno database (Huang et al, 2023), we also noticed that chromatin accessibility of the AR promoter region decreases in skin fibroblasts of aged humans compared to those of middle-aged individuals, providing a possible explanation of the age-related change in AR expression (Fig EV2M).

To investigate whether the mechanism of AR-mediated XRCC4 transcriptional regulation is conserved in mice, data mining of the previously published RNA-seq results was performed. The results revealed a positive correlation between *Ar* and *Xrcc4* mRNA levels in multiple tissues, including the lung, pancreas, and marrow, of both male and female mice (Fig 3A–F).

AR-mediated regulation of XRCC4 expression stabilizes the genome and suppresses stress-induced premature senescence

To investigate whether AR regulates genomic stability by modulating XRCC4 expression, vectors encoding XRCC4 were transfected into AR-knockdown cells, and then, a comet assay was performed (Fig 4A). The results showed that depletion of AR significantly increased the tail moment, and the increase in genomic instability could be reversed by XRCC4 overexpression (Fig 4B and C). Additionally, a similar result was obtained when genomic instability was measured by another established parameter, namely, the percentage of DNA in the tail (Fig 4D).

Since genomic instability is a causal factor of cellular senescence, we studied whether knocking down AR promotes SIPS in an XRCC4-dependent manner. AR-depleted cells or control cells were treated by X-irradiation at a dose of 10 Gy before β -gal staining to assess the degree of SIPS. We found that knocking down AR accelerated the onset of SIPS, while restoration of XRCC4 expression significantly reversed the increase in cellular senescence (Fig 4E and F). Altogether, these data confirm that AR-mediated promotion of XRCC4 expression plays an important role in regulating genomic stability and inhibiting the onset of SIPS.

DHT treatment rescues age-related XRCC4 downregulation and stabilizes the genome

It has been established that steroid hormones show age-related changes. Data mining of two independent metabolomics resources validated that the serum concentrations of multiple androgenic steroids and their derivatives markedly declined with age, in both male and female humans (Figs 5A and B, and EV3A and B) (Bucaciuc

Mracica et al, 2020; Aging Atlas Consortium, 2021). Moreover, the concentrations of androgenic hormones were decreased in plasma and several tissues in old *Macaca fascicularis* compared to young *M. fascicularis* (Fig EV3C), indicating that the alterations in levels of circulating androgenic hormones might exert a systemic effect on various tissues. Therefore, we hypothesized that androgenic steroids can be utilized to counteract the age-related decline in XRCC4 level as well as attenuate genomic instability.

DHT, which is a metabolite of testosterone, shows a very high binding affinity for AR. The binding of DHT to AR causes a conformational change in AR, leading to its nuclear translocation and binding to the promoters of its target genes (Shang et al, 2002; Schaufele et al, 2005). As expected, supplementation with DHT significantly enhanced the activity of the wild-type XRCC4 promoter but not that of the truncated promoter (Fig 5C) and increased the XRCC4 mRNA level (Fig 5D) in HCA2-hTERT cells. Furthermore, to investigate whether DHT exerts a similar effect *in vivo*, C57BL/6 mice were daily injected with DHT for 2 weeks. The data revealed a significant increase in XRCC4 mRNA levels in the skin and stomach of the DHT-injected mice (Fig EV4A and B). Employing our well-established reporter system to quantify NHEJ repair efficiency (Seluanov et al, 2004; Mao et al, 2007, 2008), we found that DHT treatment increased the NHEJ repair efficiency by 48.2% (Fig 5E and F). However, neither overexpression of XRCC4 nor DHT treatment significantly impacted HR repair efficiency (Fig EV5A and B). As a consequence, DHT treatment significantly reduced the tail moment in HCA2-hTERT cell (Fig 5G and H). Moreover, a similar result was obtained when the percentage of DNA in the tail was used as the measurement for genomic instability (Fig EV5C).

Aging is characterized by an increase in genomic instability; therefore, we examined the potential influence of DHT on genomic stability in aged cells. Aged fibroblasts were treated with DHT for 3 days, and then, RNA and protein were extracted. We found that DHT significantly increased the mRNA level of XRCC4 (Fig 5I), and the protein levels of both XRCC4 and Lig4 were markedly increased in aged fibroblasts (Fig 5J). Moreover, DHT significantly reduced the tail moment of aged cells by 61.6% (Figs 5K and EV5D), suggesting a potent effect of DHT leading the reversal of the age-associated accumulation of DNA damage.

To explore whether DHT stabilizes the genome in other types of cell models of aging, we first examined whether the AR level declines with increased cellular senescence. HCA2-hTERT cells were induced to undergo SIPS by X-irradiation. Similar to those in our experiments with aged fibroblasts, the protein levels of AR, XRCC4, and Lig4 were reduced in senescent HCA2-hTERT cells compared to nonirradiated confluent cells (Fig 5L). We then tested whether supplementation with DHT restores XRCC4 expression and stabilizes the genome in cells that had undergone SIPS. Consistently, the mRNA level of XRCC4 was significantly elevated post-DHT treatment (Fig 5M). More importantly, treating cells that had undergone SIPS with DHT for 3 days clearly reduced the tail moment (Figs 5N and EV5E), indicating that DHT treatment exerts positive effects on senescent cells.

HGPS is a rare premature aging disease (Hennekam, 2006). At the cellular level, HGPS is characterized by impaired nuclear envelope structure, accumulated DNA damage, and accelerated acquisition of senescence phenotypes (Eriksson et al, 2003). Previous studies have shown that the number of DSBs was increased in HGPS

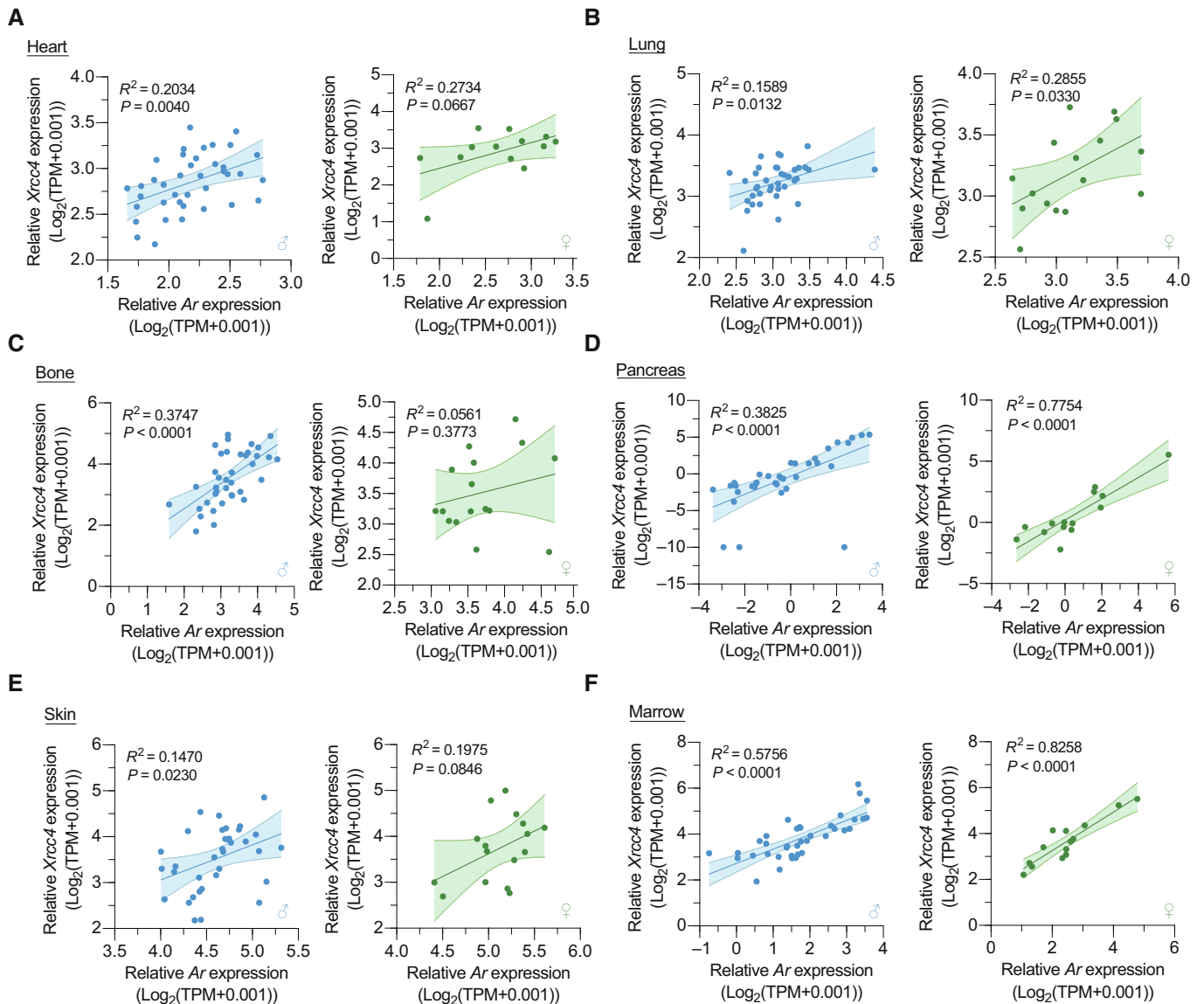


Figure 3. AR regulates XRCC4 expression in mouse tissues.

- A Correlation analysis of mRNA levels of *Ar* and *Xrcc4* in the heart of male and female mice (male, $n = 39$; female, $n = 13$).
 B Correlation analysis of mRNA levels of *Ar* and *Xrcc4* in the lung of male and female mice (male, $n = 38$; female, $n = 16$).
 C Correlation analysis of mRNA levels of *Ar* and *Xrcc4* in the bone of male and female mice (male, $n = 38$; female, $n = 16$).
 D Correlation analysis of mRNA levels of *Ar* and *Xrcc4* in the pancreas of male and female mice (male, $n = 34$; female, $n = 14$).
 E Correlation analysis of mRNA levels of *Ar* and *Xrcc4* in the skin of male and female mice (male, $n = 35$; female, $n = 16$).
 F Correlation analysis of mRNA levels of *Ar* and *Xrcc4* in the marrow of male and female mice (male, $n = 38$; female, $n = 14$). *T* test was performed to assess the significance of the regression slope in (A) to (F).

Source data are available online for this figure.

cells, implying deficient DSB repair (Liu *et al.*, 2005). Although several types of therapeutic methods have been developed, none of them were designed to target DNA repair to attenuate HGPS phenotypes. Notably, we found that the expression of AR, XRCC4, and Lig4 was decreased in HGADFN155 (HG155) cells (Fig 5O), a skin fibroblast line derived from a female HGPS patient, suggesting that DHT might also be utilized to reverse genomic instability in HGPS cells. Therefore, DHT was added to the medium of a HG155 cell culture, and we found that the mRNA level of XRCC4 was significantly

elevated (Fig 5P). DHT was also injected into the previously reported *Lmna*^{G609G/G609G} mice (Sun *et al.*, 2020), a mouse model of HGPS. Our data demonstrated that DHT administration significantly increased the XRCC4 mRNA level in the stomach and skin tissues of *Lmna*^{G609G/G609G} mice (Fig EV5F and G). Moreover, to investigate whether DHT treatment stabilized the genome, comet assay was conducted. The results revealed that the tail moment was reduced by 34.0% after 3 days of DHT treatment in HG155 cells (Figs 5Q and EV5H). Collectively, our data demonstrate that DHT effectively

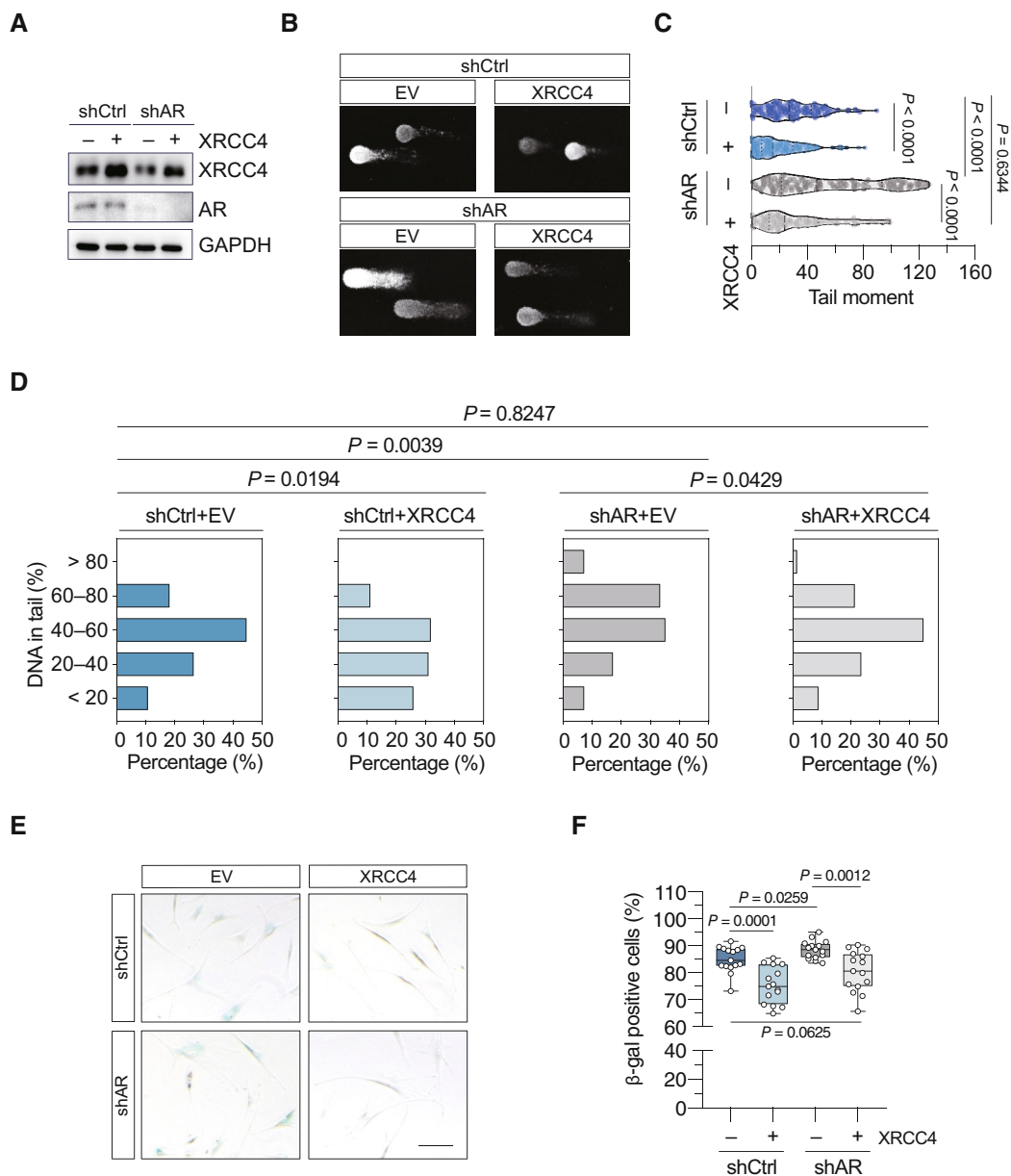


Figure 4. AR promotes XRCC4 expression to stabilize the genome and repress stress-induced premature senescence.

A XRCC4 expression analyzed with Western blot.
B–D Analysis of genomic stability in AR-depleted HCA2-hTERT cells with or without XRCC4 overexpression. Representative images of tail moment are shown in (B), the quantification of tail moment is shown in (C), and the percentages of DNA in tail are shown in (D). $n =$ at least 110 cells per group. Mann–Whitney U test was performed to determine the significance of the results presented in (C), and Chi-square test was performed to determine the significance of the results presented in (D).
E, F β -galactosidase staining of AR-depleted HCA2-hTERT cells with or without XRCC4 overexpression. Cells were treated with 10 Gy X-irradiation 24 h post-transfection and harvested for staining at 10 days post-irradiation. Representative images are shown in (E), and the quantification of β -galactosidase-positive cells is shown in (F). $n = 15$ fields per group. Scale bar: 100 μ m. Unpaired t test was performed to determine the significance of difference. Box and whisker plots indicate the median (central line), the 25th to the 75th percentiles (box), and the minimum to the maximum values (whiskers).
 Source data are available online for this figure.

attenuates the downregulation of XRCC4 and promotes genomic stability in multiple types of cell models of aging.

To investigate whether DHT promotes NHEJ repair and genomic stability in an XRCC4-dependent manner, cells expressing shRNA against XRCC4 were treated with DHT, and then, an NHEJ repair

analysis was performed. In accordance with our previous results, XRCC4 knockdown did not influence NHEJ repair efficiency (Fig 5R). This outcome might be explained by the fact that both canonical NHEJ (c-NHEJ) and alternative NHEJ (alt-NHEJ) repairs, two competitive subpathways, were detected by our reporter, and

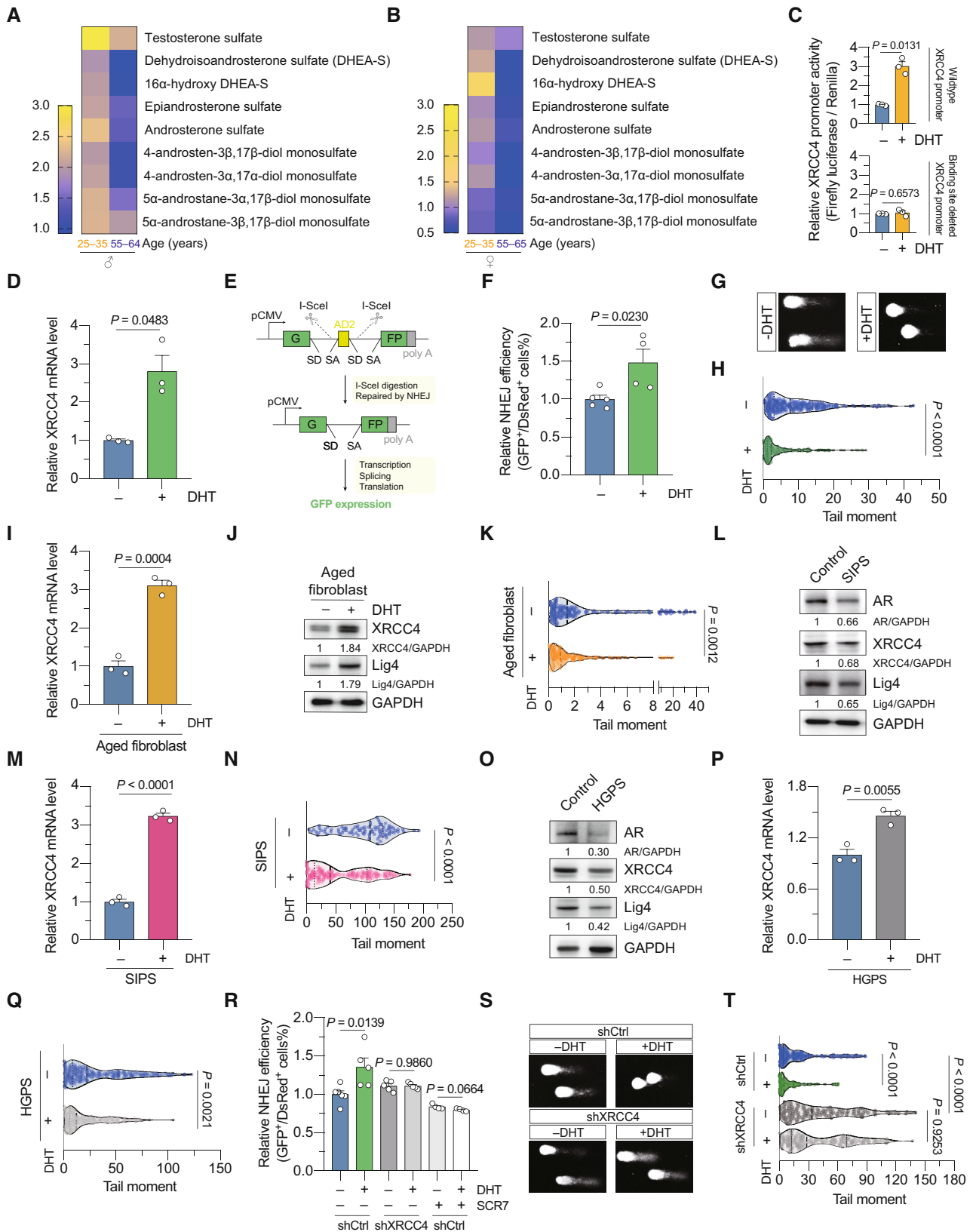


Figure 5.

Figure 5. Activation of AR with DHT restores XRCC4 expression to stabilize the genome in multiple models of cellular aging.

- A Heatmaps of androgenic steroid levels in the serum of young (25–35 years old) and aged (55–64 years old) male humans.
- B Heatmaps of androgenic steroid levels in the serum of young (25–35 years old) and aged (55–65 years old) female humans. Raw data in (A) and (B) were provided by MetaboAge database and was initially published as Saito et al (2016).
- C Effect of DHT treatment on the activity of wild-type and AR-binding site deleted XRCC4 promoter. $n = 3$ biological replicates.
- D Effect of DHT treatment on XRCC4 mRNA level. HCA2-hTERT cells were treated with 30 nM DHT for 72 h before being harvested for RNA extraction and real-time qPCR analysis. $n = 3$ biological replicates.
- E Schematic illustration of the experimental principle of NHEJ efficiency analysis.
- F Measurement of NHEJ repair efficiency in previously reported NHEJ-I9A cells treated with or without 30 nM DHT. $n = 3$ biological replicates.
- G, H Effect of DHT treatment on genomic stability. HCA2-hTERT cells were treated with 30 nM DHT for 72 h, then subjected to comet assay experiments. Representative images are shown in (G), and the tail moments were calculated and are shown in (H). Each dot represents one comet analyzed ($n =$ at least 180 cells).
- I, J Effect of DHT treatment on XRCC4 mRNA (I) and protein (J) level in the aged eyelid fibroblasts. $n = 3$ biological replicates in (I).
- K Effect of DHT treatment on genomic stability in the aged eyelid fibroblasts. Each dot represents one comet analyzed ($n =$ at least 140 cells).
- L Western blot analysis of the expression of AR, XRCC4, and Lig4 in stress-induced premature senescent (SIPS) cells. HCA2-hTERT cells were irradiated with 10 Gy X-ray to establish SIPS. Whole-cell lysates were prepared at 10 days post-irradiation.
- M Analysis of XRCC4 mRNA level in SIPS HCA2-hTERT cells treated with DHT. $n = 3$ biological replicates.
- N Effect of DHT treatment on genomic stability in SIPS HCA2-hTERT cells. SIPS HCA2-hTERT cells were treated with 30 nM DHT for 72 h, then subjected to comet assay experiments. Each dot represents one comet analyzed ($n =$ at least 90 cells).
- O Western blot analysis of the expression of AR, XRCC4, and Lig4 in the skin fibroblasts derived from an HGPS patient.
- P Effect of DHT treatment on XRCC4 mRNA in HGPS fibroblasts. $n = 3$ biological replicates.
- Q Effect of DHT treatment on genomic stability in HGPS fibroblasts. Each dot represents one comet analyzed ($n =$ at least 140 cells).
- R Analysis of the effect of DHT treatment on NHEJ repair capacity in cells with XRCC4 depleted or treated with 50 μ M SCR7. $n =$ at least four biological replicates.
- S, T Effect of DHT treatment on genomic stability in cells with XRCC4 depleted. Representative images are shown in (S), and the tail moments were calculated and are shown in (T). Each dot represents one comet analyzed ($n =$ at least 110 cells).

Error bars represent the s.e.m. values in (C), (D), (F), (I), (M), (P), and (R). Unpaired t test was performed to determine the significance of the results presented in (C), (D), (F), (I), (M), (P), and (R), and Mann–Whitney U test was performed to determine the significance of the results presented in (H), (K), (N), (Q), and (T).

Source data are available online for this figure.

although XRCC4 depletion disrupted c-NHEJ repair, the compensatory activation of alt-NHEJ enabled DNA repair. Importantly, DHT treatment significantly promoted NHEJ repair in control cells but failed to potentiate NHEJ capacity in XRCC4-knockdown cells (Fig 5R). Lig4 forms a functional ligase complex with XRCC4 and XLF during NHEJ repair. Notably, DHT did not promote NHEJ repair in cells treated with SCR7, a small-molecule inhibitor of Lig4 activity (Fig 5R). Moreover, as we reported above, DHT treatment significantly reduced the tail moment of the control cells; however, it failed to affect the genomic stability of the XRCC4-knockdown cells (Fig 5S and T). Altogether, these results demonstrate that the effect of DHT on NHEJ repair and genomic stability is dependent on XRCC4.

DHT treatment alleviates the acquisition of senescence-associated phenotypes

To further investigate whether long-term DHT treatment alleviates the acquisition senescence-associated phenotypes, the expression levels of p21 and p16, both of which participate in regulating

irreversible cell cycle arrest during cellular senescence, were analyzed by Western blotting in SIPS HCA2-hTERT cells, aged fibroblasts, and HGPS fibroblasts. We found that DHT treatment profoundly reduced the p21 level in all three cell models of aging. The p16 level was inhibited in HCA2-hTERT cells that had undergone SIPS but was marginally impacted in aged fibroblasts and HGPS fibroblasts (Fig 6A–C), in agreement with a previous finding showing that the p53-p21 axis plays a pivotal role in DNA damage-induced cellular senescence (Bunz et al, 1998). To confirm our findings, β -gal staining assays were carried out. Notably, DHT treatment led to a significant reduction in the percentage of β -gal-positive cells in the three cell models of aging (HCA2-hTERT cells after SIPS, 20.5%; aged fibroblasts, 41.4%; and HGPS cells, 14.8%) (Fig 6D–I).

Altered intercellular communication is considered a hallmark of aging, and the SASP plays an important role in intercellular interactions (Fafian-Labora & O’Loughlen, 2020). To evaluate whether DHT impacts SASP, HCA2-hTERT cells, aged fibroblasts, and HGPS cells were pretreated with DHT and then irradiated with X-rays. DHT was maintained in the culture medium post-IR. We found that 10-day DHT treatment post-irradiation significantly reduced the expression

Figure 6. DHT alleviates senescence-associated phenotypes.

- A–C Analysis of the levels of senescence markers, p21 and p16, in SIPS HCA2-hTERT cells (A), aged fibroblasts (B), and HGPS fibroblasts (C) treated with or without DHT. Cells were treated with 30 nM DHT for 10 days before being harvested for protein extraction.
- D–I β -galactosidase staining of SIPS HCA2-hTERT cells, aged fibroblasts and HGPS fibroblasts treated with or without 30 nM DHT for 10 days. Representative images are shown in (D), (F), and (H), and the quantification results are shown in (E), (G), and (I), respectively. Scale bar: 100 μ m. Unpaired t test was performed to determine the significance of the results. $n =$ at least 15 fields per group. Box and whisker plots indicate the median (central line), the 25th to the 75th percentiles (box), and the minimum to the maximum values (whiskers).
- J–O Analysis of mRNA levels of SASP factors in SIPS HCA2-hTERT cells, aged fibroblasts and HGPS fibroblasts treated with or without 30 nM DHT for 10 days. The relative expression of *IL1 β* (J), *CXCL1* (K), *CXCL2* (L), *CCL2* (M), *MMP1* (N), and *MMP3* (O) were determined by real-time qPCR with *TUBA1A* mRNA level as an internal control. Error bars in J–O represent the s.e.m. values. $n = 3$ biological replicates. Unpaired t test was performed to determine the significance of the results.

Source data are available online for this figure.

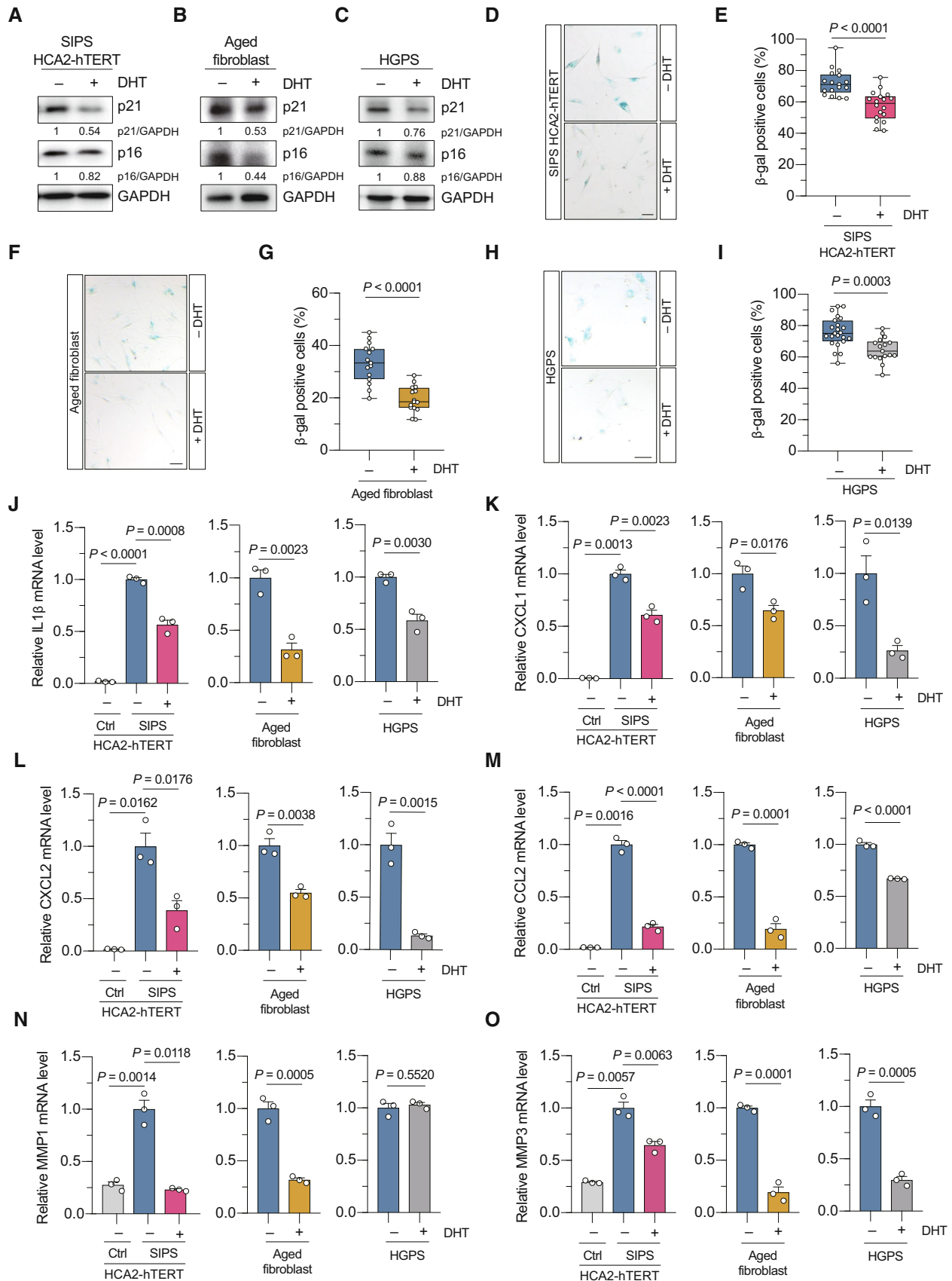


Figure 6.

level of the proinflammatory cytokine interleukin-1 β (IL1 β), which has been reported to induce DNA damage and bystander senescence in neighboring cells (Hubackova *et al*, 2012), in the HCA2-hTERT cells, aged fibroblasts, and HGPS cells (Fig 6J). However, the levels of several other cytokines, including IL1 α , IL6, and IL8, were not influenced by DHT treatment (Fig EV5I–K). C–X–C motif chemokine ligands 1 and 2 (CXCL1 and CXCL2), both of which reinforce cell cycle arrest in senescent cells (Acosta *et al*, 2008), were also significantly reduced post-DHT treatment (Fig 6K and L). Importantly, previous studies have demonstrated that C–C motif chemokine ligand 2 (CCL2) plays a role in paracrine senescence (Acosta *et al*, 2013) and recruits immunosuppressive cells to inhibit the clearance of tumor cells (Eggert *et al*, 2016), while matrix metalloproteinases 1 and 3 (MMP1 and MMP3) remodel the extracellular matrix to facilitate metastasis (Egeblad & Werb, 2002). Our data indicated that the mRNA levels of CCL2, MMP1, and MMP3 were significantly increased post-irradiation (Fig 6M–O), while DHT markedly suppressed the mRNA expression of CCL2 and MMP3 in all the aforementioned cell lines (Fig 6M and O) and reduced MMP1 levels in the HCA2-hTERT cells and aged fibroblasts (Fig 6N), implying a potent effect of DHT on mitigating the protumorigenic effects induced by senescent cells.

In summary, pharmacological activation of AR signaling with DHT represses the onset of cellular senescence and profoundly inhibits the expression of multiple SASP factors involved in senescence reinforcement, propagation, and senescence-associated tumor development.

Discussion

Aging is a systemic but nonsynchronous process that affects all organs. Aging of sex organs is considered to be the earliest event in an individual's aging. Therefore, it is possible that reproductive aging might influence the aging of other organs; however, evidence supporting this hypothesis has been lacking. Damage to macromolecules, such as DNA, is recognized as a prominent cause of aging, which is accompanied by and can be accelerated by dysregulated DNA repair. Several studies have delineated that hormone signaling pathways are involved in the regulation of DNA damage response and repair in prostate and breast cancer (Schiewer & Knudsen, 2016); however, there have been only a few studies focused on the role of hormone signaling in the interorgan regulation of DNA repair and systemic aging. Here, we showed that the expression of the sexual hormone receptor AR and the level of circulating androgenic hormones both display age-related downregulation. Impaired AR signaling contributed to the decline in NHEJ repair by downregulating the transcription of XRCC4 in aged skin fibroblasts. Nevertheless, further animal studies are required to investigate whether age-related changes in AR signaling lead to the aging of nonreproductive organs and thereby initiate aging in individuals.

An interesting question raised by our study is, why does AR expression undergo an age-associated decline, at the expense of inefficient NHEJ repair and increased rates of cellular senescence? We hypothesized that the alteration of AR signaling with age might be an example of a “lesser of two evils” mechanism. AR signaling is critical to the normal function of ovarian, uterine, and mammary glands in females (Walters *et al*, 2016), but increasing evidence has

shown that the persistent activation of AR plays profound roles in the origin and development of multiple types of tumors through distinct mechanisms, including regulatory effects on epithelial cell transformation and tumor cell proliferation, apoptosis, and migration (Chang *et al*, 2014; Pomerantz *et al*, 2015; Ma *et al*, 2021). Therefore, a gradual decline in AR signaling might exert a beneficial, antitumor effect by suppressing the aforementioned tumor promotion functions and inactivating NHEJ repair to promote irreversible cell cycle arrest in aged females. A potential paradox associated with this explanation involves the genomic instability increases cancer incidence, and a possible explanation to reconcile these conflicting outcomes is that NHEJ repair deficiency has been closely linked to premature aging phenotypes (Espejel *et al*, 2004; Li *et al*, 2007), suggesting that impaired NHEJ repair may preferentially contribute to cellular senescence, an evolutionarily conserved antitumor mechanism, preventing tumorigenesis. The regulation of AR expression at different ages might be an evolutionarily conserved mechanism to maintain a fine balance between producing offspring and surviving cancer long enough to raise offspring. Our findings are in accordance with previous findings that have led to the Grandmother hypothesis of aging (Medawar, 1952; Standen & Foley, 1989).

We report here that decreased AR transcription led to genomic instability in aged skin fibroblasts; however, what are the molecular mechanisms underlying the age-related decline in AR expression? First, the downregulation in AR expression might result from the age-related decrease in the level of androgen, a circulating sex hormone. Androgen can regulate AR expression at both the mRNA and protein levels. It increases AR mRNA levels in multiple types of cells (Kerr *et al*, 1995; Yu *et al*, 1995; Wiren *et al*, 1997); however, a report has indicated that androgen decreases the mRNA level of AR, while stabilizing AR mRNA and thus increasing AR protein expression levels (Yeap *et al*, 1999). All these prior studies indicated that an age-related decrease in androgen level may partially cause decreased AR expression in elderly individuals and further lead to a decline in XRCC4 expression and genomic stability in nonreproductive organs. Second, data mining of a previously published single-cell ATAC-seq resource (Zhang *et al*, 2021) based on the AgeAnno database (Huang *et al*, 2023) suggested that chromatin accessibility of the AR promoter region decreases in aged human skin fibroblasts compared to that in the cells of middle-aged individuals, indicating that a chromatin structure change might be another possible explanation for reduced AR expression in elderly people (Fig EV2M). Third, an increasing body of evidence has shown that the X chromosome, in which the AR gene localizes, is frequently excluded from the nucleus and is micronucleated in aged females (Guttenbach *et al*, 1994; Machiela *et al*, 2016), which might cause a reduction in AR expression. However, more data are needed to assess whether age-related X chromosome aneuploidy promotes AR downregulation.

Our work moved us one step closer to understanding the interorgan regulatory network of genomic stability and aging between reproductive and nonreproductive organs. However, future work is required to investigate whether other types of hormones and their receptors are also involved in the regulation of age-related changes in DNA repair in a tissue-specific way. Both female and male cells and animals were used in our work, and although androgenic signaling seems to exert similar regulatory functions on them, whether a sex-specific mechanism is involved remains to be determined.

Cellular senescence is characterized by the upregulation of SASP factors, many of which are proinflammatory molecules. In recent years, increasing evidence has suggested that chronic inflammation is a pillar of aging (Kennedy *et al.*, 2014). Moreover, senescent cells drive multiple age-related organ degenerative processes through the secretion of SASP factors, and senomorphics, a class of drugs that have been successfully developed to target cellular senescence by disrupting SASP (Niedernhofer & Robbins, 2018), have also exhibited great potential in treating age-related pathologies. In this study, we report that treating senescent cells with DHT, an androgenic ligand of AR, greatly attenuated the onset of senescence and reduced the levels of a list of SASP factors, including IL1 β , CXCL1, CXCL2, CCL2, MMP1, and MMP3. Although more thorough studies are needed, our results indicate that DHT might act as a novel senomorphics drug, providing an alternative strategy for senotherapy in the future.

Materials and Methods

Cell culture and transfection

All female human eyelid-derived primary cells used in this study had been described in our previous work (Li *et al.*, 2016) and were obtained with the consent of their donors and in accordance with the Ethics Committees of both Tongji University and Changzheng Hospital (2015xy111). Primary fibroblasts, HCA2-hTERT cells (previously reported in Gorbunova *et al.*, 2002), and HEK293T cells (RRID: CVCL_6911) were cultured in DMEM supplemented with 10% FBS, 1% nonessential amino acids, and 1% penicillin/streptomycin. Primary cells were maintained in a 5% CO₂ and 3% O₂ atmosphere at 37°C. All the other cells were maintained in a 5% CO₂ atmosphere at 37°C. Fibroblasts were transfected on a Lonza 4D machine with the DT-130 program. HEK293T cells were transfected with PEI reagent. Cells had not been recently authenticated. All cells were tested for mycoplasma contamination periodically and found to be mycoplasma free.

Animals

Wild-type C57BL/6 mice and *Lmna*^{G609G/G609G} mice (Sun *et al.*, 2020) were kept in a specific pathogen-free grade environment and subjected to a 12-h light/dark cycle. Mice were injected daily with either corn oil or DHT (5 mg/kg i.p., dissolved in corn oil) for a period of 2 weeks. All animal experiments were performed in compliance with the Health Guide for the Care and Use of Laboratory Animals. The animal studies were approved by the Biological Research Ethics Committee of Tongji University (TJAB04022102).

Antibodies, reagents, and plasmids

The following antibodies were used in this study: anti-XRCC4 (ABclonal, Cat. #A1677), anti-Lig4 (ABclonal, Cat. #A1743), anti-AR (Cell Signaling Technology, Cat. #5153; Abcam, Cat. #ab108341), anti-Flag tag (Sigma-Aldrich, Cat. #F3165), anti-p16 (Abcam, Cat. #ab108349), anti-p21 (Abcam, Cat. #ab109199), and anti-GAPDH (Proteintech, Cat. #60004). The following reagents were used in this study: polyethylenimine (Merck Sigma, Cat. #9002-98-6), SYBR

Green Master Mix (Roche, Cat. #A25742), DHT (APExBIO, Cat. #B8214), Pierce ECL Western blotting substrate (Thermo Scientific, Cat. #32106). The open reading frame of AR was amplified from cDNA of HCA2-hTERT cells using the following primers: AR-F, 5' ATGGAAGTGCAGTTAGGGCT 3', and AR-R 5', CTGGGTGTGGAAA TAGATGG 3'. The promoters of XRCC4 and Lig4 were amplified from the genomic DNA of HCA2-hTERT cells using the following primers: XRCC4-F, 5' CATCAGAGTTGAGACATTCAT 3', XRCC4-R, 5' CCTAATGGGATAATTTAAATCAGAAAAAG 3'; and Lig4-F, 5' GCCAGTGAGCCCCGCGACG 3', and Lig 4-R 5' ACTCGGCAA CTCCCATCACC 3'. The truncated promoter of XRCC4 was created using a ClonExpress Ultra One-Step Cloning Kit (Vazyme, Cat. # C115-01) based on the wild-type XRCC4 promoter. The sequence of shRNA directed against AR was 5' CACCAATGTCAACTCCAGGAT 3'. The sequence of the shRNA against XRCC4 was 5' GCA GCCGCTATTACCGTATCT 3'.

Chromatin immunoprecipitation (ChIP)

A ChIP assay was performed in HEK293T cells transfected with plasmid encoding Flag-tagged AR, following our previously reported procedures. Chromatin immunoprecipitation was carried out with an antibody against the Flag tag (Sigma-Aldrich, Cat. #F3165) or IgG isotype control. DNA from IP samples and input were used as templates for qPCR, and the ratio of IP-to-input DNA was calculated to be the level of relative enrichment. The following primers were used for ChIP-qPCR analysis: Primer Pair #1: F-5' GTTCCATAACTGCC ATTTC 3'; R-5' AACACAGTGAAGGAGTAGT 3'; Primer Pair #2: F-5' AGCAGACAACAGATGGAATTTACT 3'; R-5' GAACCCAGGAGG TGGAGGTT 3'; Primer Pair #3: F-5' CATCCTTAGTTATGTTGTGTTT 3'; R-5' ACAGCACTTCTGAATAGATG 3'; Primer Pair #4: F-5' AG CTTTTTGAGTCATAGTT 3'; R-5' TGTACTTATTGGAGTGGTGT 3'; Primer Pair #5: F-5' AACAAAGTAGAAAGCGGAC 3'; R-5' TAG ACTAGGGCTGGAGTTTG 3'; Primer Pair #6: F-5' CCCACTTCTTACC ATAGCGA 3'; R-5' AGCCTATCCTAGTGTCTTAAC 3'; Primer Pair #7: F-5' TGTGTTGGTTGTGGGATTGG 3'; R-5' CTCAAATTGCC TAGTACGTT 3'.

Real-time qPCR

To analyze the mRNA levels of XRCC4, Lig4, or senescence-associated secretory factors, total RNA was extracted from cells with an RNAsimple kit (TIAGEN, Cat. #DP419) and then reverse transcribed with TransScript One-Step gDNA Removal and cDNA Synthesis SuperMix (Trans, Cat. #AT311-02). Real-time qPCR was performed with SYBR Green qPCR Mix (Roche, Cat. # 04913914001) on a ViiA 7 Real-Time PCR system (Applied Biosystems). The data were analyzed using the 2^{- $\Delta\Delta C_t$} method. The following primers were used in this study: XRCC4 (human): F-5' TAAGCGGTTTA TTCTGGTGTGA 3'; R-5' CAGTTTCCCCTTCTGTTTGATG 3'; Xrcc4 (mouse): F-5' GGAGTACTGAGAGGTAGCCA 3'; R-5' TCCATA GCCATGTCATCAGC 3'; Lig4: F-5' ACAGAACACCCACTGGAAGTCA T 3'; R-5' AAGTCGTTTACTTGCTGTATGG 3'; AR (human): F-5' GAAGCTGCAAGGTCCTTCTC 3'; R-5' CCTCTCCTCTCTCTGTAGT 3'; Ar (mouse): F-5' GGACCATGTTTTACCCATCG 3'; R-5' TCGTTTC TGCTGGCACATAG 3'; GAPDH: F-5' ATGACATCAAGAGGTGGTG 3'; R-5' CATAACCAGGAAATGAGCTTG 3'; IL1 α : F-5' GGTGAGTTT AAGCCAATCCA 3'; R-5' TGCTGACCTAGGCTTGATGA 3'; IL1 β : F-5'

CTGTCTGCGTGTGAAAAGA 3'; R-5' TTGGGTAATTTTTGGGATCT ACA 3'; IL6: F-5' GCCCAGCTATGAACTCCTTCT 3'; R-5' GAAGGC AGCAGGCAACAC 3'; IL8: F-5' AGACAGCAGAGCACACAAGC 3'; R-5' ATGGTTCTTCCGGTGGT 3'; CCL2: F-5' AGTCTCTGCCGCC TTCT 3'; R-5' GTGACTGGGGCATTGATTG 3'; CXCL1: F-5' TCCTGC ATCCCCCATAGTTA 3'; R-5' CTTCAGGAACAGCCACCAGT 3'; CXC L2: F-5' CCCATGGTTAAGAAAATCATCG 3'; R-5' CTTCAGGAAC AGCCACCAAT 3'; MMP1: F-5' TTTGATGGACCTGGAGGAAAATC 3'; R-5' TGAGCATCCCCTCCAATACC 3'; MMP3: F-5' CACTCACAGACC TGACTCGTT 3'; R-5' AAGCAGGATCACAGTTGGCTGG 3'; TUBA1 α : F-5' CTTCGTCTCCGCATCAG 3'; R-5' TTGCCAATCTGGACACCA 3'.

Dual-luciferase assay

Cells cotransfected with a firefly luciferase reporter and a Renilla luciferase control vector were harvested, counted, and lysed with 200 μ l of passive lysis buffer (Promega, Cat. #E1491) per 10^6 cells for 15 min at room temperature. Ten microliters of cell lysate was mixed with 50 μ l of Dual-Glo reagent (Promega, Cat. #E1960) for analyzing the firefly luciferase activity. Then, 50 μ l of Dual-Glo Stop & Glo reagent was added to the reaction mix to analyze the Renilla luciferase activity. The dual-luciferase assay was performed with a GloMax20/20 luminometer (Promega, USA).

DHT treatment

HCA2-hTERT cells and primary fibroblasts derived from aged individuals were treated with DHT (30 nM) for 72 h, and then, the XRCC4 level was measured by real-time qPCR or Western blotting, or genomic stability analysis was performed by comet assay. Stress-induced senescent HCA2-hTERT cells and primary fibroblasts derived from aged individuals and HGPS patients were treated with DHT (30 nM) for 10 days, and then, senescence-associated markers were measured; that is, a Western blot analysis was performed to measure p16 and p21 expression levels, a β -galactosidase staining, and a real-time qPCR analysis was performed to measure SASP factor expression.

Repair efficiency analysis

NHEJ repair efficiency was analyzed with NHEJ-19A cells as previously reported (Seluanov *et al*, 2004; Mao *et al*, 2007, 2008). Briefly, 1×10^6 cells were transfected with 5 μ g of a vector encoding the I-SceI endonuclease together with 15 ng of vector encoding DsRed, which was the control for determining transfection efficiency. For the DHT experiment, cells were pretreated with DHT for 24 h before transfection, and DHT was also added in the medium post-transfection. The cells were harvested for FACS analysis 48 h post-transfection. Raw FACS data were analyzed with FlowJo software. The ratio of the percentage of GFP⁺ cells to that of DsRed⁺ cells was used as the measurement of NHEJ repair efficiency.

Comet assay

To analyze the role of AR in genomic stability maintenance, HCA2-hTERT cells with shRNA against AR or a control shRNA stably integrated into the genome were used for the comet assay, which was performed 48 h post-seeding. To analyze the effect of DHT

treatment on genomic stability, 30 nM DHT was added to the culture medium of the indicated cells, and the cells were incubated for 72 h before they were harvested for the comet assay. The comet assay was carried out according to the instructions of the manufacturer of a comet assay kit (Trevigen, Cat. #4250-050-K). The tail moment was analyzed with CaspLab software.

Senescence-associated β -galactosidase staining

Cells were treated with 30 nM DHT before being exposure to 10 Gy of X-rays. After irradiation, the culture medium was replaced, and 30 nM DHT was added to the fresh culture medium, and the cells were cultured for 10 days, when senescence-associated β -galactosidase staining was performed. The details of the procedure were previously reported (Li *et al*, 2016). Briefly, the cells were fixed in a fixation solution for 5 min and rinsed twice with PBS. Then, staining solution was added to the cells, and the cells were incubated with this stain overnight at 37°C. β -galactosidase-positive cells were counted in a blinded manner.

Statistical analyses

No statistical methods were used to predetermine sample size, and sample sizes were estimated based on experiences on the similar experiments. Simple randomization was used to allocate animals to experimental groups. The investigators were blinded to the treatment received by the cells during the analysis of the comet assay and β -galactosidase staining. Methods of statistical analysis employed to determine the significance of difference are reported in related figure legends, and the exact *P* values are indicated in figures. Prism Graph Pad (version 8) was used to perform statistical analyses.

Data availability

No large primary datasets have been generated and deposited.

Expanded View for this article is available [online](#).

Acknowledgements

We acknowledge GTEx, Tabula Muris Senis, MetaboAge, Aging Atlas, and AgeAnno database for offering publicly available resources. We thank Dr. Baohua Liu at Shenzhen University for kindly providing primary fibroblasts derived from HGPS patients. We thank Dr. Xavier Messeguer at Universitat Politècnica de Catalunya for providing kind help on transcription factor prediction with PROMO algorithm. The working model was created with [BioRender.com](#). This work was supported by the National Key R&D Program of China (2022YFA1103700 and 2021YFA1102000 to ZM), the National Natural Science Foundation of China (Grant Nos. 82225017, 32270750, and 82071565 to ZM; 81972457 and 32171288 to YJ; 32200595 to YC), and the Shanghai Sailing Program (22YF1434300 to YC).

Author contributions

Yu Chen: Conceptualization; data curation; formal analysis; supervision; funding acquisition; investigation; methodology; writing – original draft; writing – review and editing. **Zhengyi Zhen:** Data curation; formal analysis; validation; investigation; methodology; writing – review and editing.

Lingjiang Chen: Formal analysis; validation; investigation; methodology; writing – review and editing. **Hao Wang:** Formal analysis; investigation. **Xuhui Wang:** Validation; investigation. **Xiaoxiang Sun:** Validation; investigation. **Zhiwei Song:** Validation; investigation. **Haiyan Wang:** Validation; investigation. **Yizi Lin:** Validation; investigation. **Wenjun Zhang:** Investigation. **Guizhu Wu:** Investigation. **Ying Jiang:** Supervision; funding acquisition. **Zhiyong Mao:** Conceptualization; data curation; supervision; funding acquisition; project administration; writing – review and editing.

Disclosure and competing interests statement

The authors declare that they have no conflict of interest.

References

- Acosta JC, O'Loughlen A, Banito A, Gujjarro MV, Augert A, Raguz S, Fumagalli M, Da Costa M, Brown C, Popov N *et al* (2008) Chemokine signaling via the CXCR2 receptor reinforces senescence. *Cell* 133: 1006–1018
- Acosta JC, Banito A, Wuestefeld T, Georgilis A, Janich P, Morton JP, Athineos D, Kang TW, Lasitschka F, Andrulis M *et al* (2013) A complex secretory program orchestrated by the inflammasome controls paracrine senescence. *Nat Cell Biol* 15: 978–990
- Aging Atlas Consortium (2021) Aging Atlas: a multi-omics database for aging biology. *Nucleic Acids Res* 49: D825–D830
- Aging Biomarker Consortium, Bao H, Cao J, Chen M, Chen M, Chen W, Chen X, Chen Y, Chen Y, Chen Y *et al* (2023) Biomarkers of aging. *Sci China Life Sci* 66: 893–1066
- Bryans M, Valenzano MC, Stamato TD (1999) Absence of DNA ligase IV protein in XR-1 cells: evidence for stabilization by XRCC4. *Mutat Res* 433: 53–58
- Bucaciuc M, Mrcica T, Anghel A, Ion CF, Moraru CV, Tacutu R, Lazar GA (2020) MetaboAge DB: a repository of known ageing-related changes in the human metabolome. *Biogerontology* 21: 763–771
- Bunz F, Dutriaux A, Lengauer C, Waldman T, Zhou S, Brown JP, Sedivy JM, Kinzler KW, Vogelstein B (1998) Requirement for p53 and p21 to sustain G2 arrest after DNA damage. *Science* 282: 1497–1501
- Chang C, Lee SO, Yeh S, Chang TM (2014) Androgen receptor (AR) differential roles in hormone-related tumors including prostate, bladder, kidney, lung, breast and liver. *Oncogene* 33: 3225–3234
- Chen Y, Geng AK, Zhang WN, Qian Z, Wan XP, Jiang Y, Mao ZY (2020) Fight to the bitter end: DNA repair and aging. *Ageing Res Rev* 64: 101154
- Coppe JP, Desprez PY, Krtolica A, Campisi J (2010) The senescence-associated secretory phenotype: the dark side of tumor suppression. *Annu Rev Pathol* 5: 99–118
- Duncan FE, Confino R, Pavone ME (2018) Chapter 9 – Female reproductive aging: from consequences to mechanisms, markers, and treatments. In *Conn's Handbook of Models for Human Aging*, Ram JL, Conn PM (eds), 2nd edn, pp 109–130. Cambridge, MA: Academic Press
- Egeblad M, Werb Z (2002) New functions for the matrix metalloproteinases in cancer progression. *Nat Rev Cancer* 2: 161–174
- Eggert T, Wolter K, Ji J, Ma C, Yevsa T, Klotz S, Medina-Echeverz J, Longrich T, Forgues M, Reisinger F *et al* (2016) Distinct functions of senescence-associated immune responses in liver tumor surveillance and tumor progression. *Cancer Cell* 30: 533–547
- Eriksson M, Brown WT, Gordon LB, Glynn MW, Singer J, Scott L, Erdos MR, Robbins CM, Moses TY, Berglund P *et al* (2003) Recurrent de novo point mutations in lamin A cause Hutchinson-Gilford progeria syndrome. *Nature* 423: 293–298
- Espejel S, Martin M, Klatt P, Martin-Caballero J, Flores JM, Blasco MA (2004) Shorter telomeres, accelerated ageing and increased lymphoma in DNA-PKcs-deficient mice. *EMBO Rep* 5: 503–509
- Fafian-Labora JA, O'Loughlen A (2020) Classical and nonclassical intercellular communication in senescence and ageing. *Trends Cell Biol* 30: 628–639
- di Fagagna FD, Reaper PM, Clay-Farrace L, Fiegler H, Carr P, von Zglinicki T, Saretzki G, Carter NP, Jackson SP (2003) A DNA damage checkpoint response in telomere-initiated senescence. *Nature* 426: 194–198
- Farre D, Roset R, Huerta M, Adsuara JE, Rosello L, Alba MM, Messeguer X (2003) Identification of patterns in biological sequences at the ALGGEN server: PROMO and MALGEN. *Nucleic Acids Res* 31: 3651–3653
- Gladyshev VN, Kritchevsky SB, Clarke SG, Cuervo AM, Fiehn O, de Magalhães JP, Mau T, Maes M, Moritz RL, Niedernhofer LJ *et al* (2021) Molecular damage in aging. *Nat Aging* 1: 1096–1106
- Orbunova V, Seluanov A, Pereira-Smith OM (2002) Expression of human telomerase (hTERT) does not prevent stress-induced senescence in normal human fibroblasts but protects the cells from stress-induced apoptosis and necrosis. *J Biol Chem* 277: 38540–38549
- Guttenbach M, Schakowski R, Schmid M (1994) Aneuploidy and ageing: sex chromosome exclusion into micronuclei. *Hum Genet* 94: 295–298
- Hennekam RC (2006) Hutchinson-Gilford progeria syndrome: review of the phenotype. *Am J Med Genet A* 140: 2603–2624
- Hoare M, Narita M (2013) Transmitting senescence to the cell neighbourhood. *Nat Cell Biol* 15: 887–889
- Huang K, Gong H, Guan J, Zhang L, Hu C, Zhao W, Huang L, Zhang W, Kim P, Zhou X (2023) AgeAnno: a knowledgebase of single-cell annotation of aging in human. *Nucleic Acids Res* 51: D805–D815
- Hubackova S, Krejčíková K, Bartek J, Hodny Z (2012) IL1- and TGFβ₁-Nox4 signaling, oxidative stress and DNA damage response are shared features of replicative, oncogene-induced, and drug-induced paracrine 'bystander senescence'. *Ageing (Albany NY)* 4: 932–951
- Kaufman JM, Vermeulen A (2005) The decline of androgen levels in elderly men and its clinical and therapeutic implications. *Endocr Rev* 26: 833–876
- Kennedy BK, Berger SL, Brunet A, Campisi J, Cuervo AM, Epel ES, Franceschi C, Lithgow GJ, Morimoto RI, Pessin JE *et al* (2014) Geroscience: linking aging to chronic disease. *Cell* 159: 709–713
- Kerr JE, Allore RJ, Beck SG, Handa RJ (1995) Distribution and hormonal-regulation of androgen receptor (Ar) and Ar messenger-ribonucleic-acid in the rat hippocampus. *Endocrinology* 136: 3213–3221
- Kortlever RM, Higgins PJ, Bernards R (2006) Plasminogen activator inhibitor-1 is a critical downstream target of p53 in the induction of replicative senescence. *Nat Cell Biol* 8: 877–884
- Krtolica A, Parrinello S, Lockett S, Desprez PY, Campisi J (2001) Senescent fibroblasts promote epithelial cell growth and tumorigenesis: a link between cancer and aging. *Proc Natl Acad Sci USA* 98: 12072–12077
- Labrie F, Belanger A, Cusan L, Gomez JL, Candas B (1997) Marked decline in serum concentrations of adrenal C19 sex steroid precursors and conjugated androgen metabolites during aging. *J Clin Endocrinol Metab* 82: 2396–2402
- Lamberts SW, van den Beld AW, van der Lely AJ (1997) The endocrinology of aging. *Science* 278: 419–424
- Li H, Vogel H, Holcomb VB, Gu YS, Hasty P (2007) Deletion of Ku70, Ku80, or both causes early aging without substantially increased cancer. *Mol Cell Biol* 27: 8205–8214
- Li Z, Zhang W, Chen Y, Guo W, Zhang J, Tang H, Xu Z, Zhang H, Tao Y, Wang F *et al* (2016) Impaired DNA double-strand break repair contributes to the

- age-associated rise of genomic instability in humans. *Cell Death Differ* 23: 1765–1777
- Liu BH, Wang JM, Chan KM, Tjia WM, Deng W, Guan XY, Huang JD, Li KM, Chau PY, Chen DJ et al (2005) Genomic instability in laminopathy-based premature aging. *Nat Med* 11: 780–785
- Lopez-Otin C, Blasco MA, Partridge L, Serrano M, Kroemer G (2013) The hallmarks of aging. *Cell* 153: 1194–1217
- Ma M, Ghosh S, Tavernari D, Katarkar A, Clocchiatti A, Mazzeo L, Samarkina A, Epiney J, Yu YR, Ho PC et al (2021) Sustained androgen receptor signaling is a determinant of melanoma cell growth potential and tumorigenesis. *J Exp Med* 218: e20201137
- Machiela MJ, Zhou W, Karlins E, Sampson JN, Freedman ND, Yang Q, Hicks B, Dagnall C, Hautman C, Jacobs KB et al (2016) Female chromosome X mosaicism is age-related and preferentially affects the inactivated X chromosome. *Nat Commun* 7: 11843
- Mao ZY, Seluanov A, Jiang Y, Gorbunova V (2007) TRF2 is required for repair of nontelomeric DNA double-strand breaks by homologous recombination. *Proc Natl Acad Sci USA* 104: 13068–13073
- Mao ZY, Bozzella M, Seluanov A, Gorbunova V (2008) Comparison of nonhomologous end joining and homologous recombination in human cells. *DNA Repair* 7: 1765–1771
- Medawar PB (1952) *An unsolved problem of biology*. London: Published for the college by H. K. Lewis
- Messeguer X, Escudero R, Farre D, Nunez O, Martinez J, Alba MM (2002) PROMO: detection of known transcription regulatory elements using species-tailored searches. *Bioinformatics* 18: 333–334
- Niedernhofer LJ, Robbins PD (2018) Senotherapeutics for healthy ageing. *Nat Rev Drug Discov* 17: 377
- Pomerantz MM, Li FG, Takeda DY, Lenci R, Chonkar A, Chabot M, Cejas P, Vazquez F, Cook J, Shivdasani RA et al (2015) The androgen receptor cistrome is extensively reprogrammed in human prostate tumorigenesis. *Nat Genet* 47: 1346–1351
- Rodier F, Coppe JP, Patil CK, Hoeijmakers WAM, Munoz DP, Raza SR, Freund A, Campeau E, Davalos AR, Campisi J (2009) Persistent DNA damage signalling triggers senescence-associated inflammatory cytokine secretion. *Nat Cell Biol* 11: 973–979
- Saito K, Maekawa K, Kinchen JM, Tanaka R, Kumagai Y, Saito Y (2016) Gender- and age-associated differences in serum metabolite profiles among Japanese populations. *Biol Pharm Bull* 39: 1179–1186
- Schaufele F, Carbonell X, Guerbodot M, Borngraeber S, Chapman MS, Ma AA, Miner JN, Diamond MI (2005) The structural basis of androgen receptor activation: intramolecular and intermolecular amino-carboxy interactions. *Proc Natl Acad Sci USA* 102: 9802–9807
- Schiewer MJ, Knudsen KE (2016) Linking DNA damage and hormone signaling pathways in cancer. *Trends Endocrinol Metab* 27: 216–225
- Sedelnikova OA, Horikawa I, Zimonjic DB, Popescu NC, Bonner WM, Barrett JC (2004) Senescing human cells and ageing mice accumulate DNA lesions with unreparable double-strand breaks. *Nat Cell Biol* 6: 168–170
- Sedelnikova OA, Horikawa I, Redon C, Nakamura A, Zimonjic DB, Popescu NC, Bonner WM (2008) Delayed kinetics of DNA double-strand break processing in normal and pathological aging. *Aging Cell* 7: 89–100
- Seluanov A, Mittelman D, Pereira-Smith OM, Wilson JH, Gorbunova V (2004) DNA end joining becomes less efficient and more error-prone during cellular senescence. *Proc Natl Acad Sci USA* 101: 7624–7629
- Shang Y, Myers M, Brown M (2002) Formation of the androgen receptor transcription complex. *Mol Cell* 9: 601–610
- Standen V, Foley R (1989) *Comparative socioecology: the behavioural ecology of humans and other mammals*. Oxford; Boston; Brookline Village, MA: Blackwell Scientific Publications; Publisher's Business Services distributor
- Sun S, Qin W, Tang X, Meng Y, Hu W, Zhang S, Qian M, Liu Z, Cao X, Pang Q et al (2020) Vascular endothelium-targeted Sirt7 gene therapy rejuvenates blood vessels and extends life span in a Hutchinson-Gilford progeria model. *Sci Adv* 6: eaay5556
- Walters KA, Simanainen U, Gibson DA (2016) Androgen action in female reproductive physiology. *Curr Opin Endocrinol* 23: 291–296
- Wang CF, Jurk D, Maddick M, Nelson G, Martin-Ruiz C, von Zglinicki T (2009) DNA damage response and cellular senescence in tissues of aging mice. *Aging Cell* 8: 311–323
- White BA, Porterfield SP (2013) Introduction to the endocrine system. In *Endocrine and Reproductive Physiology*, 4th edn, pp 1–e2. Philadelphia, PA: Mosby
- Wiren KM, Zhang XW, Chang CS, Keenan E, Orwoll ES (1997) Transcriptional up-regulation of the human androgen receptor by androgen in bone cells. *Endocrinology* 138: 2291–2300
- Yeap BB, Krueger RG, Leedman PJ (1999) Differential posttranscriptional regulation of androgen receptor gene expression by androgen in prostate and breast cancer cells. *Endocrinology* 140: 3282–3291
- Yu LQ, Nagasue N, Makino Y, Nakamura T (1995) Effect of androgens and their manipulation on cell-growth and androgen receptor (Ar) levels in Ar-positive and Ar-negative human hepatocellular carcinomas. *J Hepatol* 22: 295–302
- Yu QJ, Katlinskaya YV, Carbone CJ, Zhao B, Katlinski KV, Zheng H, Guha M, Li N, Chen QJ, Yang T et al (2015) DNA-damage-induced type I interferon promotes senescence and inhibits stem cell function. *Cell Rep* 11: 785–797
- Zhang H, Cai B, Geng A, Tang H, Zhang W, Li S, Jiang Y, Tan R, Wan X, Mao Z (2020) Base excision repair but not DNA double-strand break repair is impaired in aged human adipose-derived stem cells. *Aging Cell* 19: e13062
- Zhang K, Hocker JD, Miller M, Hou X, Chiou J, Poirion OB, Qiu Y, Li YE, Gaulton KJ, Wang A et al (2021) A single-cell atlas of chromatin accessibility in the human genome. *Cell* 184: 5985–6001